Bioresource Technology 304 (2020) 123016

Contents lists available at ScienceDirect

Bioresource Technology

journal homepage: www.elsevier.com/locate/biortech

Effects of different conductive nanomaterials on anaerobic digestion process and microbial community of sludge

Yawen Chen[a,b], Zhaohui Yang[a,b,*], Yanru Zhang[a,b], Yinping Xiang[a,b], Rui Xu[c], Meiying Jia[a,b], Jiao Cao[a,b], Weiping Xiong[a,b]

[a] *College of Environmental Science and Engineering, Hunan University, Changsha 410082, PR China*
[b] *Key Laboratory of Environmental Biology and Pollution Control (Hunan University), Ministry of Education, Changsha 410082, PR China*
[c] *Guangdong Key Laboratory of Integrated Agro-environmental Pollution Control and Management, Guangdong Institute of Eco-environmental Science Technology, Guangzhou 510650, PR China*

GRAPHICAL ABSTRACT

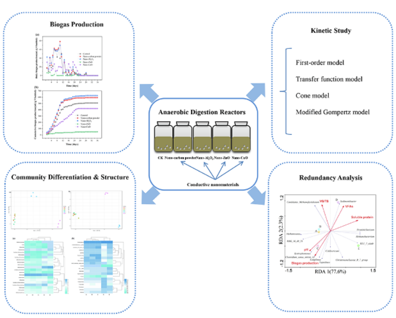

ARTICLE INFO

Keywords:
Anaerobic digestion
Conductive nanomaterials
Waste activated sludge
Kinetic model
Microbial community

ABSTRACT

The effects of four conductive nanomaterials (nano-carbon powder, nano-Al_2O_3, nano-ZnO, nano-CuO) on sludge anaerobic digestion (AD) performance and microbial community were investigated through a 36-day fermentation experiment. Results showed that biogas production enhanced by 16.9% and 23.4% with nano-carbon powder and nano-Al_2O_3 added but decreased by 90.2% and 17.3% with nano-ZnO and nano-CuO. Total solids (TS) removal efficiency was increased by 38.73% and 27.11% with nano-carbon powder and nano-Al_2O_3 added but decreased by 70.67% and 43.70% with nano-ZnO and nano-CuO. Kinetic analysis indicated four conductive nanomaterials could shorten the lag phase of AD sludge with an average rate of 51.75%. 16S rRNA amplicon sequencing results demonstrated microbes such as *Syntrophomonas* and *Methanosaeta* were enriched in nano-carbon powder and nano-Al_2O_3 reactors. However, microbial community diversity and richness were both inhibited by adding nano-ZnO and nano-CuO. Redundancy analysis (RDA) revealed that genera belong to *Firmicutes* and *Chloroflexi* could conduce to methanogenesis process.

1. Introduction

The amount of sewage in urban sewage treatment plants has increased annually, and huge amounts of waste activated sludge (WAS) have been waited to be disposed (Wu et al., 2018). Anaerobic digestion (AD) is one of the important methods to stabilize, reduce and recycle

* Corresponding author at: College of Environmental Science and Engineering, Hunan University, Changsha 410082, PR China.
E-mail address: yzh@hnu.edu.cn (Z. Yang).

https://doi.org/10.1016/j.biortech.2020.123016
Received 24 December 2019; Received in revised form 8 February 2020; Accepted 11 February 2020

sludge in sewage treatment plant. However, there were still some known disadvantages of AD, such as low degradation rate of organic matter and long reaction time. Therefore, scholars have constantly worked on sludge AD to increase the production rates of methane and boost AD performance. The technologies to improve AD performance of sludge mainly including pretreating sludge, anaerobic co-digestion (Elalami et al., 2019) and adding additives etc.

Adding additives has become a widely used approach to improve sludge AD performance. Among the additives, nanomaterials have been the most dominant additives to enhance AD performance currently (Romero-Güiza et al., 2016). Some of the nanomaterials possessed larger specific surface area and better electron conductivity, which could enhance extracellular electron transport between exoelectrogenic bacteria and methanogenic archaea, thereby promoting methane production more effectively (Roco, 2005). Nano-Al_2O_3, carbon based nanomaterials, nano-ZnO and nano-CuO are common industrial additives and have broad application prospects. Many researchers have focused on the effects of nanomaterials on AD performance. Carbon based nanoparticles (NPs) have been increasingly applied in AD, some studies have found that conductive carbon based NPs such as graphene and carbon nanotubes could promote the start-up of thermophilic process and promote direct interspecies electron transfer (DIET) between microorganisms, and then the efficiency of anaerobic reactions could be enhanced (Yan et al., 2017). It has been reported that nano-Al_2O_3 possessed a positive effect on methane generation, but the reason was unclear (Kökdemir Ünşar and Perendeci, 2018).

The influences of nano-ZnO and nano-CuO on AD process have also been investigated by previous studies. Mu et al. (2011) found that all the dosage of ZnO NPs possessed significant inhibition effect on methane production apart from the dosage of it was less than 6 mg g^{-1} TSS. Zhang et al. (2017) evaluated the influences of ZnO nanomaterials on volatile fatty acids (VFA) accumulation in sludge AD. They found that ZnO nanomaterials showed negative impacts on the VFA consumption and biogas production. Previous study revealed that the addition of CuO NPs could cause obvious negative influence on the microbial richness, diversity and composition of WAS in sequencing batch reactor activated sludge process (SBR) (Wang et al., 2017). Thus, the dissolved metal ions released from oxides might be a possible reason for CuO NPs and ZnO NPs influencing AD performance and the variations of microbial community structure (Jiang et al., 2009). And it can be inferred that the enhancement of WAS biogas production might be related to DIET. From what has been discussed above, the effects of different conductive nanomaterials on AD process were different. Some effects were positive, others were negative, which was dominantly related to the properties and dosage of nanomaterials. It is known that researchers have focused on the effects of conductive nanomaterials on AD to produce methane, but the influences of conductive nanomaterials on microbial community structure have less been explored.

In recent years, scholars have paid more attention to the study of digestion kinetic characteristics. The study of kinetic modeling was conducive to predict the process and behavior of AD system, and then optimized the AD process. The parameters of kinetic models could reveal the kinetic mechanisms of AD process instability or stability (Kainthola et al., 2019). There has been study evaluated the correlation of kinetic parameters with operational conditions and process performance of co-anaerobic digestion of food waste (Li et al., 2018). However, the influence on the kinetic parameters with conductive nanomaterials adding to sludge AD system has not yet been fully explored.

The purpose of this study was to investigate the effects of four conductive nanomaterials (nano-carbon powder, nano-Al_2O_3, nano-ZnO, nano-CuO) on anaerobic digestion process and microbial community of sludge. This study aimed to (i) understand how the four conductive nanomaterials affected AD process. Main attention was given to the parameters which can present performance and stability of AD, including biogas production, organic matter removal efficiency, pH, changes of intermediate products (concentration/composition of volatile fatty acids (VFAs), soluble protein and soluble polysaccharide); (ii) predict biogas production potential, and to investigate the influence on kinetic parameters with the addition of four conductive nanomaterials to AD system through kinetic study; (iii) evaluate the microbial community structure of sludge in response to different conductive nanomaterials added through 16S rRNA amplicon sequencing, then to find out the nanomaterials with the obvious disturbance to microbial community structure among the four conductive nanomaterials; (iv) analyze the correlation between the microbial community and environmental factors for sludge samples. The results were expected to provide a research basis for evaluating the influence of conductive nanomaterials on anaerobic digestion process of sludge.

Table 1
Main characteristics of seed sludge and feed sludge used in this study.

Item	Seed sludge	Feed sludge
TS (g L^{-1} substrate)	30.3 ± 1.9	90.7 ± 6.5
VS (g L^{-1} substrate)	10.0 ± 0.8	35 ± 2.5
VS/TS (%)	33.0 ± 1.4	38.6 ± 0.2
sCOD (mg L^{-1})	605.0 ± 131.3	3617. 1 ± 298.0
pH	7.58 ± 0.1	6.3 ± 0.1
VFAs(mg L^{-1})	31.6 ± 20.5	204.9 ± 146.8

2. Materials and methods

2.1. Sewage sludge samples and conductive nanomaterials

The dewatered sludge and WAS were both collected from Kaifu District Waste Water Treatment Plant (Changsha, China). Main characteristics of sludge were summarized in Table 1. The WAS was acclimated in a constant temperature incubator at 35 °C for a month to obtain the seed sludge. The feed sludge was a mixture of WAS and dewatered sludge in equal proportion. The four conductive nanomaterials, nano-carbon powder (99.5%, 30 nm), nano-Al_2O_3 (99.9% metals basis, 30 nm), nano-ZnO (99.9% metals basis, 30 nm) and nano-CuO (99.5%, 40 nm) were all purchased from Macklin biochemical technology co. LTD, Shanghai, China.

2.2. Anaerobic digestion reactors set-up and operation

Experiment was conducted in 15 glass reactors with a working volume of 3.0 L, the mixture of 2.0 L seed sludge and 1.0 L feed sludge was added into the reactors as the substrate of AD. Before the reaction began, nitrogen gas was aerated to each reactor for 15 min to ensure the anaerobic condition. The experiment was conducted in a constant temperature water bath at 35 °C for 36 days. The experiment was set as five reactors, the control reactor (A), which were same as other reactors but without adding conductive nanomaterial, nano-carbon powder reactor (B), nano-Al_2O_3 reactor (C), nano-ZnO reactor (D) and nano-CuO reactor (E), the dosage of four conductive nanomaterials reactors were all 50.0 mg g^{-1} TS. Three parallel samples were set for each reactor.

2.3. Analytical methods

pH, soluble protein, soluble polysaccharide, soluble chemical oxygen demand (sCOD), TS, volatile solids (VS) and ammonia nitrogen (NH_4^+-N) were measured followed the standard methods (Eaton et al., 1995). The VFAs were measured using a gas chromatograph (HP5890, USA). The analytical methods of these have all been described in previous literatures (Xu et al., 2018a, 2019). The daily biogas production was measured by water-replace method. All experiments were conducted in triplicates.

Table 2
Models used for the kinetic study to analyze the cumulative biogas production.

Model	Equation	Parameters
Modified Gompertz model	$B_t = B_0 \exp\left\{-\exp\left[\frac{R_m * e}{B_0} * (\lambda - t) + 1\right]\right\}, \quad t \geq 0$	R_m, B_0, λ
Cone model	$B_t = \frac{B_0}{1 + (k * t)^{-n}}, \quad t > 0$	B_0, k, n
Transfer function model	$B_t = B_0 * \left\{1 - \exp\left[\frac{-R_m * (t - \lambda)}{B_0}\right]\right\}, \quad t \geq 0$	R_m, B_0, λ
First-order kinetic model	$B_t = B_0 * [1 - \exp(-k * t)], \quad t \geq 0$	B_0, k

B_t: cumulative biogas production at t days of digestion time (mL g^{-1} VS_{added}); B_0: the biogas production potential (mL g^{-1} VS_{added}); R_m: maximum biogas production rate (mL g^{-1} VS d^{-1}); λ: lag phase (d); t: the time of AD (d); n: shape factor; k: hydrolysis rate constant (day^{-1}); e = 2.7183.

2.4. Kinetic models

In order to predict biogas production potential, and to investigate the influence on kinetic parameters with the addition of four conductive nanomaterials to AD system, the Modified Gompertz model, Cone model, transfer function model and first-order kinetic model were used for the kinetic study to analyze the cumulative biogas production (Table 2).

2.5. 16S rRNA amplicon sequencing

Each reactor was sampled and lyophilized for 16S rRNA amplicon sequencing on the 36th day. An extraction kit (Bioteke Corporation, Beijing, China) was applied to extract the microbial DNA. The V4-V5 region of the archaeal 16S rRNA gene was amplified via polymerase chain reaction (PCR) with primer set 524F (5′-TGY CAG CCG CCG CGG TAA-3′)/958R (5′-YCC GGC GTT GAV TCC AAT T-3′) for sample identification. And the V3-V4 region of the bacterial 16S rRNA gene was amplified via PCR with primer set 338F (5′-ACT CCT ACG GGA GGC AGC A-3′)/806R (5′-GGA CTA CHV GGG TWT CTA AT-3′) for sample identification. Then the Illumina pair-ended sequencing was performed on the Illumina MiSeq-PE250 platform (Xu et al., 2018b). Sequencing raw data were deposited to NCBI, the submission ID is SUB5914270.

2.6. Statistical analysis

The Origin 2018 software was used to analyze the kinetic models and draw graphs. The Hemi 1.0 software was used to produce heat map. Correlation between microbial community and environment factors was assessed by Redundancy analysis (RDA) with the Canoco 4.5 (Microcomputer Power, USA).

3. Results and discussion

3.1. Effects of different conductive nanomaterials on AD performance

3.1.1. Change of biogas production

Daily biogas production of five reactors was within the range of 0–78.46 mL g^{-1} VS_{added} (Fig. 1 (a)). And daily biogas production of five reactors were within the range of 0–62.71 (control), 0–78.46 (nano-carbon powder), 0–69.77 (nano-Al_2O_3), 0–9.97 (nano-ZnO) and 0–31.43 (nano-CuO) mL g^{-1} VS_{added}, respectively. Among them, the daily biogas production of nano-carbon powder reactor and nano-Al_2O_3 reactor were higher than control reactor, but nano-ZnO reactor and nano-CuO reactor had lower daily biogas production than control reactor. Daily biogas production was relatively low in all reactors before the 10th day. And at about the 10th day, daily biogas production of control, nano-carbon powder and nano-Al_2O_3 reactors reached a peak. As shown in Fig. 1(b), the cumulative biogas production of nano-carbon powder and nano-Al_2O_3 reactors were obviously higher than that of control reactor in the initial ten days. After 36-day experiment, the

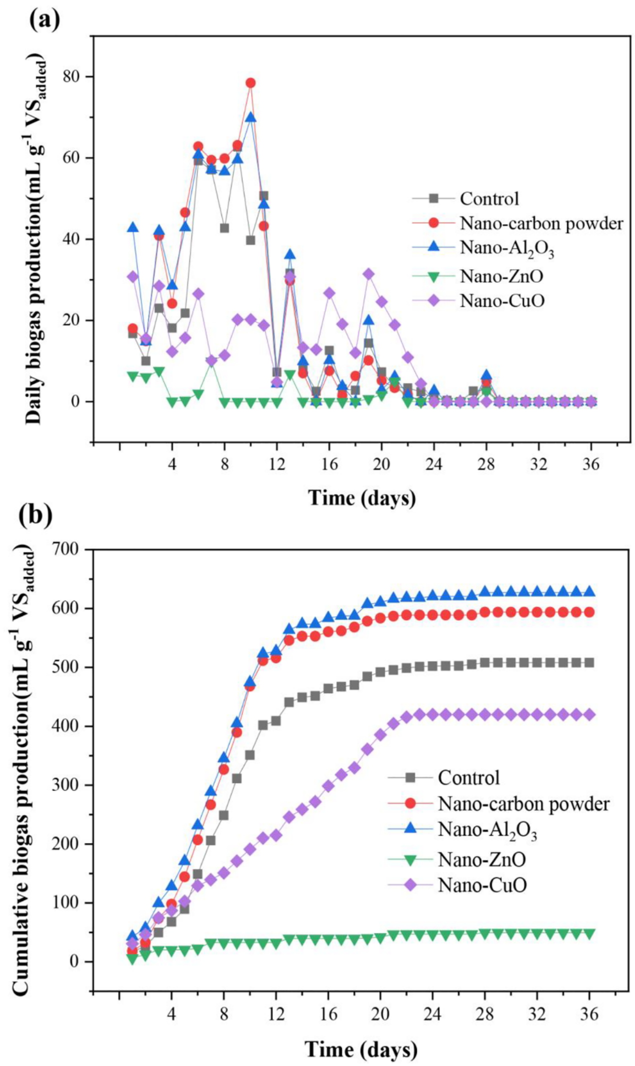

Fig. 1. Daily biogas production (a) and cumulative biogas production (b) during AD in different reactors.

cumulative biogas production of five different reactors were 508.12 (control), 593.94 (nano-carbon powder), 627.11 (nano-Al_2O_3), 49.57 (nano-ZnO) and 420.03 (nano-CuO) mL g^{-1} VS_{added}, respectively. And cumulative biogas production was followed the order of nano-Al_2O_3 > nano-carbon powder > control > nano-CuO > nano-ZnO. Compared with the biogas production in control reactor, the biogas production increased by 16.9% and 23.4% in nano-carbon powder reactor and nano-Al_2O_3 reactor, respectively, but decreased by 90.2% and 17.3% in nano-ZnO reactor and nano-CuO reactor, respectively. The results above showed that the addition of nano-Al_2O_3 and nano-carbon powder could promote the biogas production of AD, especially nano-Al_2O_3 could maximize the cumulative biogas production of AD, while, the addition of nano-ZnO and nano-CuO could significantly inhibit biogas production.

DIET was superior to interspecies electron transfer (IET) which used diffusive electron carrier such as H_2 or formate (Rotaru et al., 2014). It have been reported that DIET between electron-donating bacteria and methane-forming archaea could be enhanced by carbon based nanomaterials added, the conversion of carbon dioxide to methane was promoted, lag time for initiating biogas production was reduced, and methane production was enhanced (Park et al., 2018). Therefore, in this study, the large surface area of nano-carbon powder promoted more efficient microorganism attachment. Moreover, it promoted DIET between exoelectrogenic bacteria and methanogenic archaea (Barua and Dhar, 2017). DIET was faster than IET thus the addition of nano-carbon powder possessed a positive impact on biogas generation. Fewer previous studies have investigated the effects of adding nano-Al_2O_3 on sludge AD. Yang et al. (2012) reported that nano-Al_2O_3 had no toxic effects on the methanogenic activity, and even showed a positive effect on it, which was because of the weak solubility of nano-Al_2O_3. The results demonstrated that nano-Al_2O_3 possessed a positive effect on biogas production of AD, and this was because the large surface area and appropriate pore structure of nano-Al_2O_3, which provided a good carrier for anaerobic medium (Kökdemir Ünşar and Perendeci, 2018).

It was reported that nano-ZnO showed larger inhibitory effect on methane generation with its dosages increased (Mu and Chen, 2011). Applerot et al. (2009, 2012) studied that CuO NPs and ZnO NPs for the toxicity mechanism of bacteria, and their results showed that NPs would adsorb on the cell surface, and the NPs that suspended in the water would produce reactive oxygen species (ROS) with water (CuO NPs mainly produced superoxide anions and ZnO NPs mainly produced hydroxyl radicals). In addition, nanoparticles with smaller particle size would produce more active oxides. Oxidative stress induced cell at the same time, a part of CuO NPs and ZnO NPs with smaller particle size infiltrated into cells and eventually caused cell damage. Therefore, based on the results obtained, toxic Cu^{2+} and Zn^{2+} ions released from nano-CuO and nano-ZnO induced the increase of intracellular ROS (Xia et al., 2008). Then, the increase of intracellular ROS can lead to cell membrane damage and cytoplasmic leakage of bacteria. Besides, increased ROS possessed toxicity to protein and other intermediates in cell, which can also explain why nano-CuO and nano-ZnO made adverse impacts on AD process in this study, especially the impacts on methane generation.

3.1.2. Removal of organic matter

The removal efficiency of sCOD, TS and VS are all significant parameters which usually used to evaluate the efficiency of AD (Zhen et al., 2016). As shown in Fig. 2(a), the TS removal efficiency of five reactors were 36.04% (control), 50.00% (nano-carbon powder), 45.81% (nano-Al_2O_3), 10.57% (nano-ZnO) and 20.29% (nano-CuO), respectively. The VS removal efficiency of five reactors were 52.39% (control), 72.16% (nano-carbon powder), 60.74% (nano-Al_2O_3), 30.08% (nano-ZnO) and 44.53% (nano-CuO), respectively. Compared

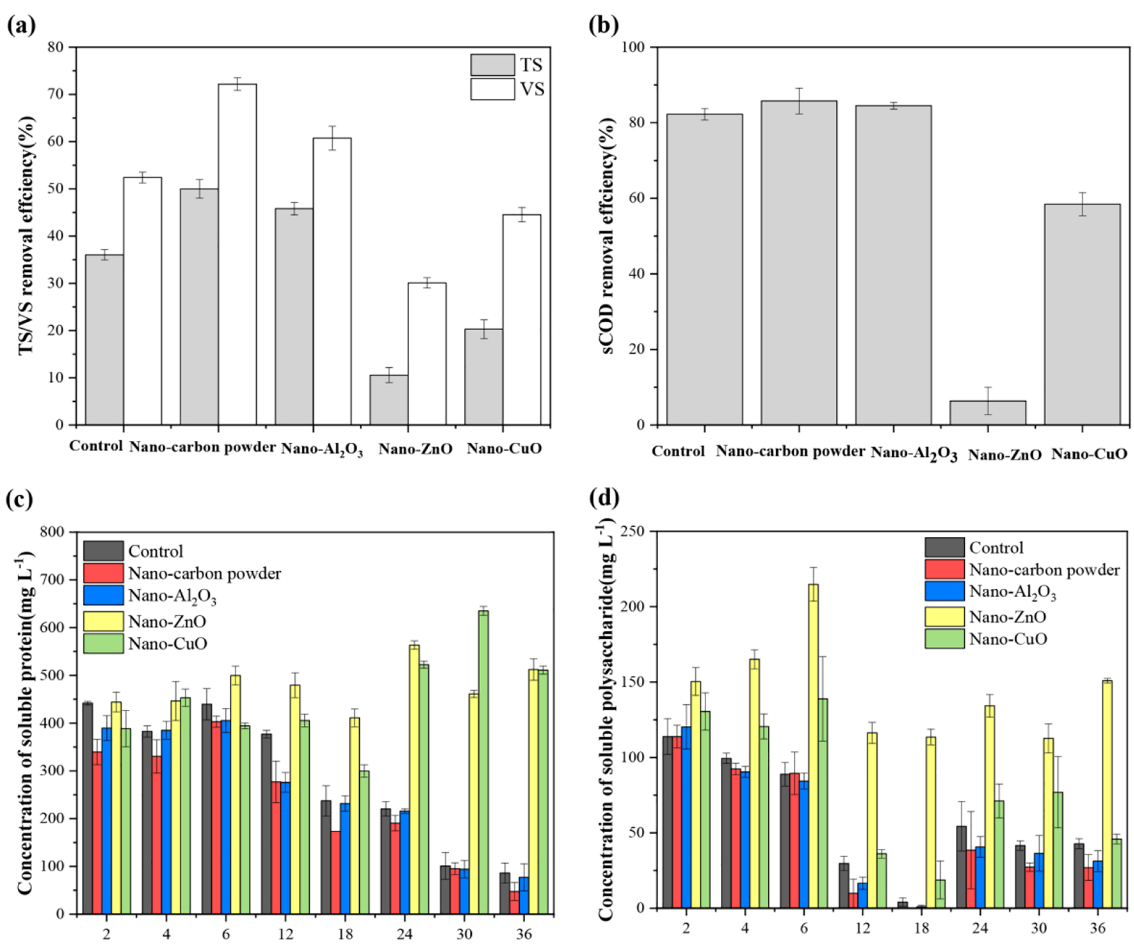

Fig. 2. TS/VS removal efficiency (a) and sCOD removal efficiency (b) of sludge in different reactors after experiments. Changes of soluble protein (c) and soluble polysaccharide (d) during AD in different reactors.

with the control reactor, TS removal efficiency increased 38.73% and 27.11% in nano-carbon powder and nano-Al_2O_3 reactors, respectively. VS removal efficiency increased 37.74% and 15.94% in nano-carbon powder and nano-Al_2O_3 reactors, respectively. The results suggested that the addition of nano-carbon powder and nano-Al_2O_3 did enhance TS and VS removal efficiencies. However, TS and VS removal efficiencies were both decreased with the addition of nano-CuO and nano-ZnO. The removal efficiency of sCOD were 82.24% (control), 85.74% (nano-carbon powder), 84.49% (nano-Al_2O_3), 6.37% (nano-ZnO) and 58.45% (nano-CuO), respectively (Fig. 2(b)). Compared with the control reactor, sCOD removal ratio of nano-carbon powder and nano-Al_2O_3 reactors increased 4.26% and 2.74%, respectively. However, the sCOD removal ratio of nano-ZnO reactor was decreased 92.25%.

The results above demonstrated that the addition of nano-carbon powder and nano-Al_2O_3 could enhance TS, VS and sCOD removal efficiencies, indicating that nano-carbon powder and nano-Al_2O_3 stimulated the activity of anaerobic microorganisms via DIET thereby promoted the degradation of organic matter (Xu et al., 2015). However, adding nano-CuO and nano-ZnO made negative impacts on organic matter removal efficiency. Toxic Cu^{2+} and Zn^{2+} ions which released from nano-CuO and nano-ZnO damaged the cell membrane of anaerobic bacteria, and then anaerobic bacterial activity was reduced, even caused some anaerobic microbial death. It was an important reason for the low degradation of organic matter (Neal, 2008). High organic matter removal efficiency represented the acceleration of methanogenic process. Generally, biogas production was related to the removal of organic matter during AD process, thus the results of biogas production were similar to the results of organic matter removal.

3.1.3. Change of soluble protein and soluble polysaccharide

Soluble protein and soluble polysaccharide are both solubilized products of hydrolysis, which could represent the degree of sludge hydrolysis. Fig. 2(c) and (d) showed the changes of soluble protein and soluble polysaccharide in different reactors during 36-day experiment. The degradation efficiency of soluble protein in five reactors were 92.81% (control), 96.03% (nano-carbon powder), 93.57% (nano-Al_2O_3), 57.24% (nano-ZnO) and 57.33% (nano-CuO), respectively. Nano-carbon powder and nano-Al_2O_3 reactors released 3.47% and 0.82% more soluble protein than the control reactor, respectively. The degradation efficiency of soluble polysaccharide in five reactors were 88.67% (control), 92.87% (nano-carbon powder), 91.74% (nano-Al_2O_3), 60.06% (nano-ZnO) and 87.87% (nano-CuO), respectively. The degradation ratio of soluble polysaccharide in nano-carbon powder and nano-Al_2O_3 reactors increased 4.74% and 3.46% than the control reactor, respectively. However, the degradation efficiency of these two solubilized products of hydrolysis in nano-ZnO and nano-CuO reactors were both much lower than control reactor. Based on the results obtained, the change of soluble protein and soluble polysaccharide concentration showed the similar trend with organic matter removal behavior.

In this study, the high degradation ratio of soluble protein and soluble polysaccharide in nano-carbon powder and nano-Al_2O_3 reactors was because that these two materials could enhance the activity of anaerobic microorganisms (Zhen et al., 2015). Furthermore, it was found that adding conductive nanomaterials to AD reactors could promote the formation of micro-electrolysis systems, and the degradation of total polysaccharide and granular proteins could be enhanced rapidly (Feng et al., 2015). Therefore, the decomposition of sludge promoted effectively. However, Gonzalez-Estrella et al. (2013) found that the degradation efficiency of soluble protein and soluble polysaccharide showed a decrease trend with the increase of nano-ZnO dosage, which was due to its inhibition impacts on hydrolysis. Protease and cellulase are both key enzymes during hydrolysis stage (Mu and Chen, 2011), they play important roles in hydrolyzing soluble protein and soluble polysaccharide. This study found that adding nano-ZnO and nano-CuO made an inhibitory effect on degradation ratio of soluble protein and soluble polysaccharide, the possible reason was that activities of protease and cellulose were inhibited by adding nano-ZnO and nano-CuO. It can be preliminarily judged that the inhibitory effect of nano-ZnO and nano-CuO on the hydrolysis of soluble protein and polysaccharide might be one of the reasons for declined methane production.

3.1.4. Change of VFAs and pH

pH is often used to evaluate the stability of AD system (Xiang et al., 2019). The pH value has a great influence on the activity of methanogens in AD system, and the optimum pH range for their survival is 6.8–7.2 (Zhao et al., 2018). The pH values of five reactors were within the range of 6.7–7.5, they did not change much. Accordingly, concentration of $NH_4{}^+$-N didn't change much either. The pH value of nano-carbon powder reactor was higher than other four reactors, which was possibly because that carbon based nanomaterial could alleviate the impact of acid to wastewater and WAS in anaerobic digesters (Xu et al., 2015). The variations of total VFAs concentration (acetic acid, propionic acid, n-butyric acid, iso-butyric acid, n-valeric acid and iso-valeric acid) during 36-day AD were showed in Fig. 3. Total VFAs concentration of control and nano-carbon powder reactors were rapidly peaked on the sixth day, and then rapidly dropped after the sixth day. Nevertheless, total VFAs concentration of nano-Al_2O_3 reactor basically showed a downward trend. As the anaerobic reaction progressed, the VFAs concentration of nano-ZnO and nano-CuO reactors increased gradually.

Biogas generation was directly connected with the presence of VFAs in anaerobic reactor (Zhang et al., 2018). The accumulation of VFAs in AD reactor could reflect the inactive state of methanogens and the deterioration of the reactor's operating conditions, higher VFAs concentration could inhibit the methanogens. Thus, with the accumulation of VFAs in control and nano-carbon powder reactors, especially the generation of acetic acid in the early stage of anaerobic reaction (before the sixth day), biogas production didn't increase either. After the sixth day, VFAs in control, nano-carbon powder and nano-Al_2O_3 reactors were all consumed in large quantities, the concentration of VFAs decreased rapidly, and pH value rose steadily, thereby all of which provided a comfortable living environment for methanogens. Therefore, biogas production also enhanced greatly. The inhibition to the consumption of n-butyric acid and iso-butyric acid in nano-ZnO and nano-CuO reactors might because that these two nanomaterials could inhibit the metabolic pathway of butyric acid to acetic acid. With the accumulation of VFAs concentration in nano-ZnO and nano-CuO reactors, the content of acetic acid in total VFAs was high, biogas production of these two reactors didn't increase either. The results were same as Mu et al. (2011), their study revealed that inhibition impact of nano-ZnO on methane generation was probably because nano-ZnO significantly inhibited the bio-conversion process of acetic acid to methane. Besides, VFAs were dominantly produced from degrading soluble protein and soluble polysaccharide. Therefore, the inhibitory impact on the soluble protein and soluble polysaccharide degradation with nano-ZnO and nano-CuO added was the possible reason for the slow production and consumption of VFAs.

3.2. Kinetic study of cumulative biogas production

Cone model and Modified Gompertz model were used for the kinetic study to analyze the cumulative biogas production of each reactor. According to the data in Tables 3 and 4, it can be observed that cumulative biogas production was well fitted by these two models, R^2 were both more than 0.96 and within the range of 0.96–0.99. The estimated kinetic parameters were summarized in Tables 3 and 4.

The maximum biogas production rate (R_m) can be used to evaluate the methane production of different AD reactors. In general, the larger value of R_m, the higher methane production of the reactors (Zhang et al., 2019). As shown in Table 3, R_m of five reactors were 52.40

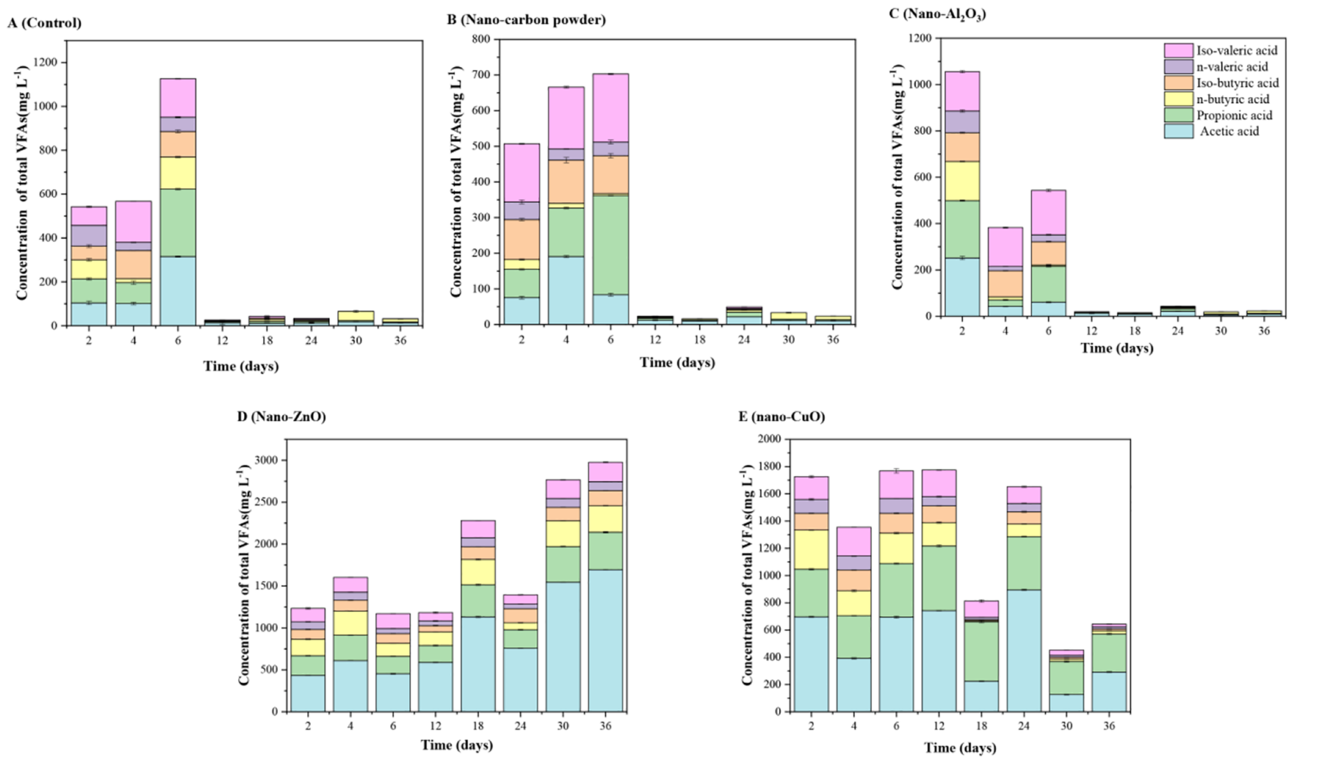

Fig. 3. Changes of total VFAs during AD in different reactors.

Table 3
Parameters of Modified Gompertz model obtained from the cumulative biogas production.

Reactors	B_0	R_m	λ	R^2	Difference (%)
Control	505.79	52.40	3.01	0.9975	6.18
Nano-carbon powder	593.01	68.02	2.80	0.9964	5.93
Nano-Al_2O_3	626.76	61.89	2.02	0.9961	4.61
Nano-ZnO	50.19	2.42	0.12	0.9614	0
Nano-CuO	451.76	21.81	0.87	0.9852	5.54

Table 4
Parameters of Cone model obtained from the cumulative biogas production.

Reactors	B_0	k	n	R^2	Difference (%)
Control	515.11	0.1271	3.17587	0.9972	7.96
Nano-carbon powder	601.40	0.1393	3.27944	0.9947	8.30
Nano-Al_2O_3	641.90	0.1407	2.75522	0.9923	7.85
Nano-ZnO	68.03	0.0663	0.88261	0.9738	4.81
Nano-CuO	430.67	0.0767	1.67334	0.9735	10.99

(control), 68.02 (nano-carbon powder), 61.89 (nano-Al_2O_3), 2.42 (nano-ZnO) and 21.81 (nano-CuO) mL g^{-1} VS d^{-1}, respectively. R_m in nano-carbon powder and nano-Al_2O_3 reactors were increased by 29.8% and 23.4% more than control reactor, respectively, but decreased by 95.38% and 58.38% in nano-ZnO and nano-CuO reactors, respectively. The value of kinetic parameters was similar to the experimental value. B_0 gotten from Cone model and Modified Gompertz model were both followed the same order, which was followed the order of nano-Al_2O_3 > nano-carbon powder > control > nano-CuO > nano-ZnO. It was consistent with the experimental data, demonstrating the addition of nano-carbon powder and nano-Al_2O_3 did have positive impacts on biogas production. The calculated lag phase (λ) indicated the period required for the microorganisms in the anaerobic system to acclimate the new environment (Zhang et al., 2014). From Table 3, the calculated lag phase (λ) value was the highest in control reactor, and this was mainly due to the excellent conductivity of the four conductive nanomaterials (Park et al., 2018). Besides, these four conductive nanomaterials could promote synthesizing the enzymes and cell constituents required for active growth, thus they shortened the calculated lag phase (λ) of AD sludge and promoted the reaction rate of AD. As shown in Table 4, hydrolysis rate constant (k) represented the hydrolysis rate of sludge during AD, the magnitude of its value indicated the degradation rate of hydrolysis (Zhen et al., 2015). From the result analyzed by Cone model, k value of five reactors were 0.1271 (control), 0.1393 (nano-carbon powder), 0.1407 (nano-Al_2O_3), 0.0663 (nano-ZnO) and 0.0767 (nano-CuO) day^{-1}, respectively. k value of nano-carbon powder and nano-Al_2O_3 reactors increased from 0.1271 to 0.1393 day^{-1}, and 0.1271 to 0.1407 day^{-1} compared with the control reactor, respectively. This apparently demonstrated that the addition of nano-carbon powder and nano-Al_2O_3 indeed enhanced the hydrolysis rate. The possible reason for it was that adding nanomaterials to AD reactors could form the micro-electrolysis systems thereby accelerating the hydrolysis of sludge matrix (Feng et al., 2015).

3.3. Microbial community of sludge in response to different conductive nanomaterials added

3.3.1. Variation of microbial community composition at different taxonomy level

For the purpose of evaluating the effects of adding different conductive nanomaterials on microbial community structure, the species composition and distribution of microbial community at phylum and genus level were analyzed. As shown in Fig. 4(a), the archaeal community in five reactors mainly included four phyla. *Euryarchaeota* was the most abundant phylum of all phyla in each reactor, the relative abundance of it in control, nano-carbon powder, nano-Al_2O_3 and nano-CuO reactors reached over 97%, however, that in nano-ZnO reactor was the lowest, which was mainly because of the addition of nano-ZnO made its activity inhibited. Previous studies found that *Crenarchaeota* possessed the function of ammoxidation key function (amoA) and the potential for ammonia oxidation (Ding et al., 2015). The relative

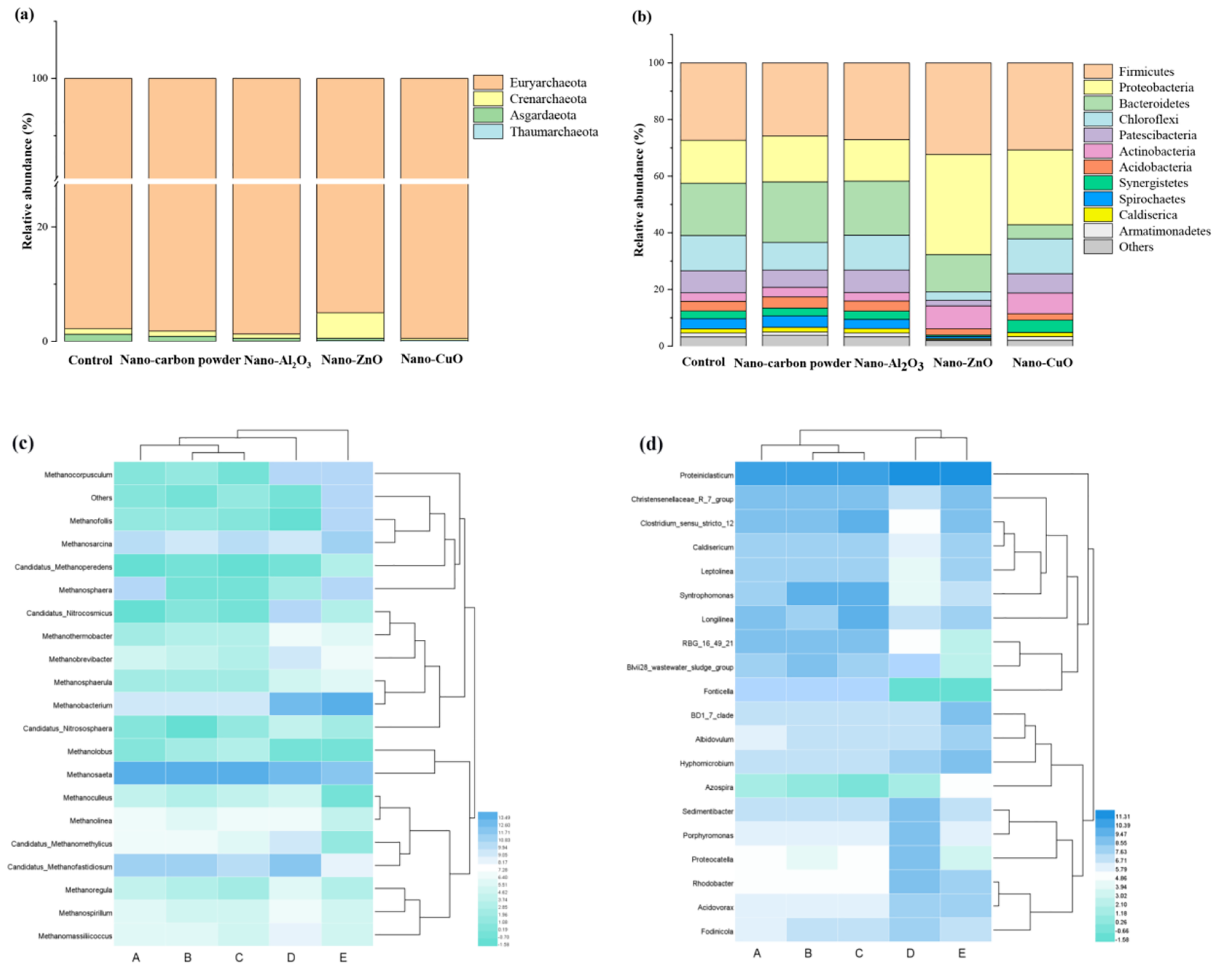

Fig. 4. Archaeal (a) and bacterial (b) community structure at phylum level of sludge in different reactors. Heat map demonstrated the evolution of archaea (c) and top 20 bacteria (d) at genus level in five reactors during AD. The color intensity showed the relative abundance of each genus as the color key indicated at the bottom right.

abundance of *Crenarchaeota* obviously increased in nano-ZnO reactor, demonstrating that the activity of *Crenarchaeota* could be enhanced by nano-ZnO added.

As shown in Fig. 4(b), the bacterial community in five reactors was mainly included eleven phyla. The dominant phyla of bacterial community in five reactors were *Chloroflexi*, *Bacteroidetes*, *Proteobacteria and Firmicutes*, these four phyla were all dominant phyla of AD (Nelson et al., 2011), they accounted for 68% to 77% of the total bacterial community. Compared with the control reactor, *Proteobacteria* increased in nano-ZnO and nano-CuO reactor. The relative abundance of *Bacteroidetes* in five reactors were 18.49%, 21.37%, 19.08%, 13.15% and 4.91%, respectively. And *Chloroflexi* decreased about 75.64% in nano-ZnO reactor against with the control reactor. *Firmicutes* can be widely found in AD systems, it contained many significant functional microorganisms and played an important role during AD process. *Proteobacteria* was involved in the degradation of organic matter in AD system, it can induce cell lysis and release intracellular substances (Cheng et al., 2018). The increased abundance of *Proteobacteria* in nano-ZnO and nano-CuO reactors may be the adaptation and resistance to the addition of these two nanomaterials to AD system. Members of *Bacteroidetes* played a crucial role in hydrolyzing polysaccharide (Vanwonterghem et al., 2014). Adding nano-carbon powder and nano-Al_2O_3 made the content of *Bacteroidetes* increased, which was because these two nanomaterials promoted the hydrolysis of polysaccharide. *Chloroflexi* can produce hydrolytic enzymes to degrade soluble microbial products which included soluble protein and soluble polysaccharide etc. (Cheng et al., 2018). The relative abundance of *Chloroflexi* decreased in nano-ZnO reactor against with the control reactor, attributing to the great inhibition of nano-ZnO to the hydrolysis of soluble protein and soluble polysaccharide.

The heat map (Fig. 4(c)) demonstrated the evolution of archaeal in genus during AD in five reactors, the archaeal community in five reactors mainly included 20 genera. *Methanosaeta*, *Methanobacterium* and *Candidatus_Methanofastidiosum* were the top 3 abundant genera in all reactors. *Methanosaeta* was the most dominant genus, the relative abundance of it in five reactors were 79.26%, 80.33%, 84.96%, 45.84% and 22.70%, respectively. And the relative abundance of *Methanobacterium* in five reactors were 2.49%, 2.79%, 2.71%, 27.34% and 65.24%, respectively. *Methanosaeta* is a significant methanogenic archaea. And it is a strictly methanogen of acetic acid type that possessed a higher affinity for acetic acid (Jetten et al., 1991). The decrease of *Methanosaeta* in nano-ZnO and nano-CuO reactors indicated that adding these two nanomaterials could inhibit the activity of *Methanosaeta*. The lowest relative abundance of *Methanobacterium* was in control reactor suggested that the presence of conductive nanomaterials probably promoted the growth of *Methanobacterium*, which was agreed with the study of Liu et al. (2015). An obvious fluctuation of *Methanobacterium* relative abundance could be observed in nano-ZnO and nano-CuO reactors, which was due to the stress behavior exhibited by the AD system on the invasion of external ZnO NPs and CuO NPs. *Methanosarcina* and *Methanosaeta* are both methanogens of acetic acid type. The bigger abundance of *Methanosarcina*, the less abundance of *Methanosaeta* can be observed when adding four conductive nanomaterials. This demonstrated that these two methanogens possessed competitive relationship. The low biogas production in nano-ZnO and nano-CuO reactors was possibly because of the variations in the structure of archaea community.

Fig. 4(d) demonstrated the evolution of bacterial in genus during AD in five reactors, top 20 abundant genera were selected to analyze. *Proteiniclasticum* was the most dominant genus in each reactor. *Clostridium_sensu_stricto_12* and *Longilinea* in nano-Al_2O_3 reactor were both higher than others. The content of *Clostridium_sensu_stricto_12*, *Syntrophomonas*, *Caldisericum* and *Leptolinea* were all dropped in nano-ZnO reactor compared with the control reactor. The members of *Proteiniclasticum* could utilize tryptone to produce acetic acid and they might be related to DIET (Yin et al., 2017; Zhang et al., 2009). *Syntrophomonas* and *Clostridium_sensu_stricto_12* belong to *Firmicutes*. *Longilinea* belongs to *Chloroflexi*. *Clostridium_sensu_stricto_12* and *Longilinea* in nano-Al_2O_3 reactor were both higher than other reactors, these two genera were closely related to the consumption of VFAs (Zheng et al., 2018), which can be used to explain why the VFAs concentration in nano-Al_2O_3 reactor dropped rapidly. *Syntrophomonas* is an acetogen that consumed butyrate, which plays an important role in long-chain fatty acids degradation (Sousa et al., 2007). An obvious drop of its relative abundance in nano-ZnO reactor indicated that the activity of *Syntrophomonas* was inhibited with nano-ZnO added. Besides, *Syntrophomonas* plays an important role in acetogenesis and could promote the transfer of electrons to methanogens (Saha et al., 2019). The addition of nano-carbon powder and nano-Al_2O_3 facilitated an increase in the relative abundance of the *Syntrophomonas*, which was the possible reason for the enhancement of biogas production. Previous studies found that several species included in *Clostridium* are cellulolytic bacteria, which of them are important participants of cellulose degradation (Burrell et al., 2004). The result demonstrated that the activity of *Clostridium_sensu_stricto_12* was inhibited with the presence of nano-ZnO, which was related to the low degradation of soluble polysaccharide in nano-ZnO reactor. *Clostridium_sensu_stricto_12*, *Syntrophomonas*, *Caldisericum* and *Leptolinea* were all involved in the degradation of macromolecular compounds in methane-producing biological systems. It reflected that toxic ions released from nano-ZnO inhibiting the activity of these genera, then caused negative impacts on organic matter removal efficiency. From what has been discussed above, it can be concluded that the addition of conductive nanomaterials did change the microbial abundance and structure.

3.3.2. Diversity analysis of microbial community

Table 5 showed the Alpha-diversity indices of microbial community in five reactors. Four kinds of indices which can reflect the richness and inter-species diversity of community were mainly be analyzed and compared. The bacterial observed species number was followed the order of control > nano-Al_2O_3 > nano-carbon powder > nano-CuO > nano-ZnO, the highest number of bacterial observed species (2104), Chao 1 index (2430.96), and ACE index (2460.51) were all in control reactor, indicating that the richness of bacterial community decreased in the presence of four conductive nanomaterials. Specifically, these four conductive nanomaterials probably disturbed the bacterial dynamics. However, the highest number of Shannon index and Simpson index were both observed in nano-carbon powder reactor. It obviously demonstrated that the addition of nano-carbon powder can enhance diversity of bacterial community. Nevertheless, four indices of bacterial community in nano-ZnO and nano-CuO reactors were whole lower than other reactors, indicating that the bacterial community was relatively lower diversity and richness with nano-ZnO and nano-CuO added. This is mainly related to toxic Cu^{2+} and Zn^{2+} ions released from nano-CuO and nano-ZnO, which damaged cell membrane of bacteria, and reduced the activity of bacteria, then made negative effects on the richness and diversity of bacterial community.

As for archaeal community, compared with control reactor, higher number of observed species and four indices were found in nano-carbon powder and nano-Al_2O_3 reactors, which was consistent with the observed biogas production. It demonstrated that the addition of nano-carbon powder and nano-Al_2O_3 possessed positive impacts on archaeal community. However, nano-ZnO reactor possessed the lowest number of observed species (695), Chao 1 index (776.57), ACE index (774.36), Shannon index (2.84) and Simpson index (0.798), demonstrating that the presence of nano-ZnO possessed the greatest negative effect on the richness and diversity of archaeal community in sludge AD system. In conclusion, there were indeed some different effects on the richness and diversity of microbial community with the addition of different conductive nanomaterials.

Beta diversity refers to the difference in species composition between different reactors. Principal coordinates analysis (PCoA) was adopted to evaluate differences in microbial community composition between different reactors (Fig. 5). The percentage (Axis-1 and Axis-2) represented the proportion of the difference in the original data that the corresponding principal coordinate can explain. The first and the second ordination axes could explain 78.1% and 14.4% of archaea, respectively. And they could explain 60.3% and 22.5% of bacteria, respectively. It can be observed that five reactors were roughly divided into three parts, the distance between the control, nano-carbon powder and nano-Al_2O_3 reactors was very close. Nevertheless, nano-ZnO and nano-CuO reactor were both far away from the other three reactors. The results revealed that the structure of microbial community among control, nano-carbon powder and nano-Al_2O_3 reactor was more similar, and the difference was smaller. However, the influence on the bacterial and archaeal composition with the accumulation of nano-CuO and nano-ZnO in AD system was different from that with nano-carbon powder and nano-Al_2O_3. Heavy metal compounds such as CuO and ZnO are hard to be biodegraded, thereby they may accumulate and reach the potentially toxic concentrations for bacteria finally. The possible reason for this result was nano-CuO and nano-ZnO possessed the function to induce the toxicity towards the microorganisms and damage the microbial cytomembrane. Therefore they made an obvious influence on the microbial richness, diversity and composition of sludge during AD. Furthermore, there was also difference between nano-CuO and nano-ZnO reactors' microbial community structure. This was dominantly because that nano-ZnO possessed higher solubility than nano-CuO in sludge (Luna-delRisco et al., 2011; Wang et al., 2017).

Table 5
Alpha-diversity indices of bacterial and archaeal community of different reactors.

Reactors	Observed species		Chao 1 index		ACE index		Shannon index		Simpson index	
	Bacterial	Archaeal	Bacterial	Archaeal	Bacterial	Archaeal	Bacterial	Archaeal	Bacterial	Archaeal
Control	2104	779	2430.96	894.34	2460.51	920.02	6.08	3.12	0.989	0.842
Nano-carbon powder	2050	830	2341.89	965.67	2368.14	978.91	6.11	3.23	0.990	0.848
Nano-Al_2O_3	2099	819	2403.55	957.13	2429.58	971.80	6.08	3.15	0.989	0.845
Nano-ZnO	1520	695	1697.86	776.57	1709.19	774.36	5.67	2.84	0.983	0.798
Nano-CuO	1590	709	1863.37	788.90	1863.18	794.87	5.37	2.92	0.959	0.811

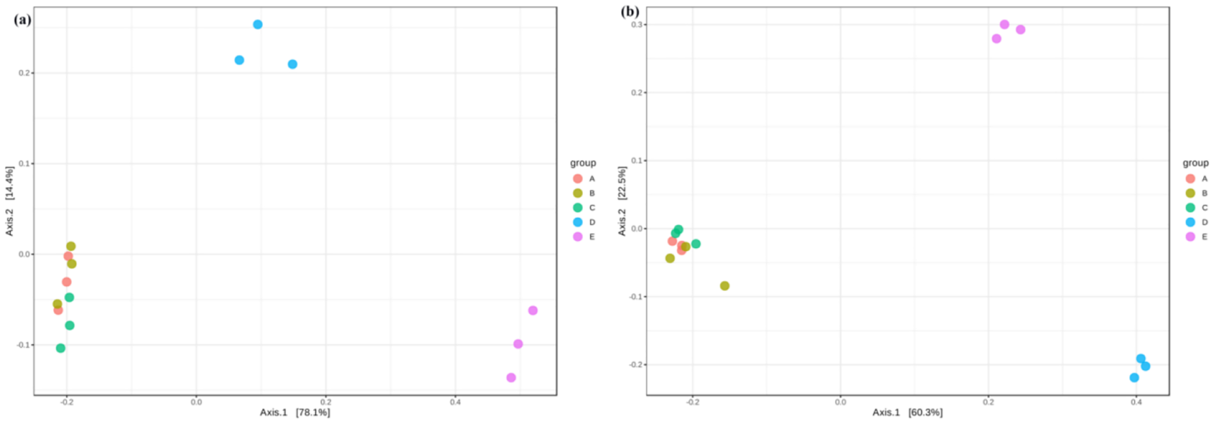

Fig. 5. Principal coordinates analysis: archaeal (a) and bacterial (b) PCoA based on the normalized OTU table, and different colored point represents different reactors, plotted by the second principal component on the Axis-2 and the first principal component on the Axis-1.

3.4. Correlation between microbial community and environment factors

The correlation between the microbial community and the reactors' performance was analyzed by Redundancy analysis (RDA). Five parameters of AD system including pH, VFAs, biogas production, soluble protein and VS/TS were subjected to Redundancy analysis together with the 13 microbes at genus level in the sludge samples (top 10 genera of bacteria and top 3 genera of archaea). The first and the second ordination axes could explain 77.6% and 2.3% of the microbial community variations, respectively. As shown in Fig. 6, the microorganisms were approximately divided into three parts, first part of the microorganisms were related to VS/TS, the second part of them were related to VFAs and soluble protein, the third part of them were related to pH and biogas production. It can be observed that the differences between sludge samples of nano-carbon powder, nano-Al_2O_3 reactor and control reactor were relatively small, while the differences between sludge samples of nano-ZnO, nano-CuO reactor and control reactor were relatively large, the result was consistent with the result of Beta diversity analysis. There was strong relationship between *Methanosaeta* and biogas production while *Methanobacterium* did not show positive response to biogas production. *Clostridium_sensu_stricto_12*, *Leptolinea*, *Syntrophomonas* and *Longilinea* showed obviously relationship with pH and biogas production. Moreover, *Sedimentibacter* was strongly associated with VFAs. The strong relationship between *Methanosaeta* and biogas production indicated that *Methanosaeta* was crucial in methanogenesis process. *Clostridium_sensu_stricto_12* and *Syntrophomonas* belong to *Firmicutes*. *Longilinea* and *Leptolinea* belong to *Chloroflexi*. It was reported that *Firmicutes* and *Chloroflexi* were both dominant microorganisms in AD system and were significant for the generation of biogas (Wei et al., 2017). In this study, *Clostridium_sensu_stricto_12*, *Leptolinea*, *Syntrophomonas* and *Longilinea* all showed positive correlation with biogas production, proving these microorganisms conduced to the methanogenesis process. Moreover, *Sedimentibacter* was closely related to VFAs, which was because *Sedimentibacter* was associated with the consumption of VFAs.

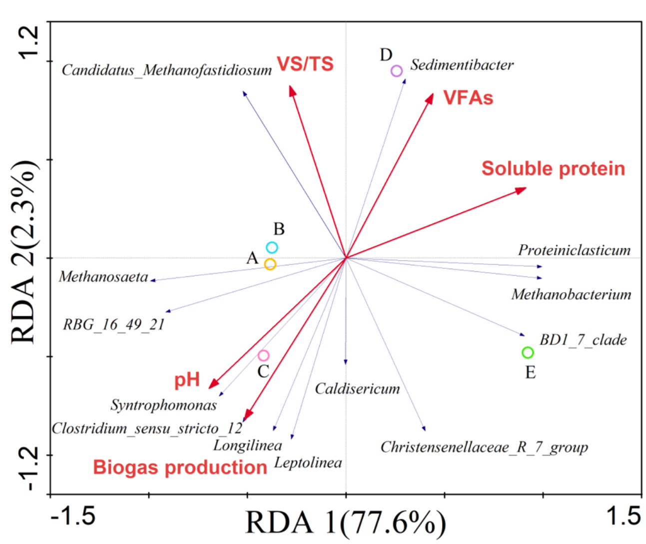

Fig. 6. Redundancy analysis revealed the correlation between the microbial community and environmental factors for sludge samples. Top 10 bacterial and top 3 archaeal at genus level of each reactor were selected. Different color of circles represents different reactors.

4. Conclusions

Biogas production, TS and VS removal efficiency of AD could be enhanced by adding nano-carbon powder and nano-Al_2O_3 but inhibited by nano-ZnO and nano-CuO. Kinetic analysis indicated that all conductive nanomaterials could shorten the lag phase of AD sludge. Microbes such as *Syntrophomonas* and *Methanosaeta* were enriched in nano-carbon powder and nano-Al_2O_3 reactors. Evidently negative effects were showed on microbial community diversity and richness by adding nano-ZnO and nano-CuO, which caused inhibitory impacts on AD performance. The analysis of correlation between microbial community and environment factors demonstrated that genera which belong to *Firmicutes* and *Chloroflexi* could conduce to methanogenesis process.

Acknowledgements

This work was supported by the National Natural Science Foundation of China (51878258 and 51521006) and the Key Research and Development Program of Hunan Province (2017SK2242).

Declaration of Competing Interest

The authors declare that they have no known competing financial interests or personal relationships that could have appeared to influence the work reported in this paper.

Appendix A. Supplementary data

Supplementary data to this article can be found online at https://doi.org/10.1016/j.biortech.2020.123016.

References

Applerot, G., Lipovsky, A., Dror, R., Perkas, N., Nitzan, Y., Lubart, R., Gedanken, A., 2009. Enhanced antibacterial activity of nanocrystalline ZnO due to increased ROS-mediated cell injury. Adv. Funct. Mater. 19 (6), 842–852.

Applerot, G., Lellouche, J., Lipovsky, A., Nitzan, Y., Lubart, R., Gedanken, A., Banin, E., 2012. Understanding the antibacterial mechanism of CuO nanoparticles: revealing the route of induced oxidative stress. Small (Weinheim an der Bergstrasse, Germany) 8.

Barua, S., Dhar, B.R., 2017. Advances towards understanding and engineering direct interspecies electron transfer in anaerobic digestion. Bioresour. Technol. 244, 698–707.

Burrell, P.C., O'Sullivan, C., Song, H., Clarke, W.P., Blackall, L.L., 2004. Identification, detection, and spatial resolution of Clostridium populations responsible for cellulose degradation in a methanogenic landfill leachate bioreactor. Appl. Environ. Microbiol. 4 (70).

Cheng, C., Zhou, Z., Qiu, Z., Yang, J., Wu, W., Pang, H., 2018. Enhancement of sludge reduction by ultrasonic pretreatment and packing carriers in the anaerobic side-stream reactor: performance, sludge characteristics and microbial community structure. Bioresour. Technol. 249, 298–306.

Ding, L., Liu, Z., Aggrey, M., Li, C., Chen, J., Tong, L., 2015. Nanotoxicity: the toxicity research progress of metal and metal- containing nanoparticles. Mini-Rev. Med. Chem. 15, 529–542.

Eaton, A.D., Greenberg, A.E., Clesceri, L.S., Franson, M.A.H., 1995. Standard Methods for the Examination of Water & Wastewater.

Elalami, D., Carrere, H., Monlau, F., Abdelouahdi, K., Oukarroum, A., Barakat, A., 2019. Pretreatment and co-digestion of wastewater sludge for biogas production: recent research advances and trends. Renew. Sustain. Energy Rev. 114, 109287.

Feng, Y., Zhang, Y., Chen, S., Quan, X., 2015. Enhanced production of methane from waste activated sludge by the combination of high-solid anaerobic digestion and microbial electrolysis cell with iron–graphite electrode. Chem. Eng. J. 259, 787–794.

Gonzalez-Estrella, J., Sierra-Alvarez, R., Field, J.A., 2013. Toxicity assessment of inorganic nanoparticles to acetoclastic and hydrogenotrophic methanogenic activity in anaerobic granular sludge. J. Hazard. Mater. 260, 278–285.

Jetten, M., Stams, A.J.M., Zehnder, A.J.B., 1991. Methanogenesis from acetate: a comparison of the acetate metabolism in Methanothrix soehngenii and Methanosarcina sp. FEMS Microbiol. Rev. 88 (1992), 181–198.

Jiang, W., Mashayekhi, H., Xing, B., 2009. Bacterial toxicity comparison between nano- and micro-scaled oxide particles. Environ. Pollut. 157 (5), 1619–1625.

Kainthola, J., Kalamdhad, A.S., Goud, V.V., 2019. Enhanced methane production from anaerobic co-digestion of rice straw and hydrilla verticillata and its kinetic analysis. Biomass Bioenergy 125, 8–16.

Kökdemir Ünşar, E., Perendeci, N.A., 2018. What kind of effects do Fe2O3 and Al2O3 nanoparticles have on anaerobic digestion, inhibition or enhancement? Chemosphere 211, 726–735.

Li, L., He, Q., Zhao, X., Wu, D., Wang, X., Peng, X., 2018. Anaerobic digestion of food waste: correlation of kinetic parameters with operational conditions and process performance. Biochem. Eng. J. 130, 1–9.

Liu, Y., Zhang, Y., Ni, B.-J., 2015. Zero valent iron simultaneously enhances methane production and sulfate reduction in anaerobic granular sludge reactors. Water Res. 75, 292–300.

Luna-delRisco, M., Orupõld, K., Dubourguier, H.-C., 2011. Particle-size effect of CuO and ZnO on biogas and methane production during anaerobic digestion. J. Hazard. Mater. 189 (1), 603–608.

Mu, H., Chen, Y., Xiao, N., 2011. Effects of metal oxide nanoparticles (TiO2, Al2O3, SiO2 and ZnO) on waste activated sludge anaerobic digestion. Bioresour. Technol. 102 (22), 10305–10311.

Mu, H., Chen, Y., 2011. Long-term effect of ZnO nanoparticles on waste activated sludge anaerobic digestion. Water Res. 45 (17), 5612–5620.

Neal, A., 2008. What can be inferred from bacteria-nanoparticle interactions about the potential consequences of environmental exposure to nanoparticles? Ecotoxicology (London, England) 17, 362–371.

Nelson, M.C., Morrison, M., Yu, Z., 2011. A meta-analysis of the microbial diversity observed in anaerobic digesters. Bioresour. Technol. 102 (4), 3730–3739.

Park, J.-H., Kang, H.-J., Park, K.-H., Park, H.-D., 2018. Direct interspecies electron transfer via conductive materials: a perspective for anaerobic digestion applications. Bioresour. Technol. 254, 300–311.

Roco, M.C., 2005. The emergence and policy implications of converging new technologies integrated from the nanoscale. J. Nanopart. Res. 7 (2), 129–143.

Romero-Güiza, M.S., Vila, J., Mata-Alvarez, J., Chimenos, J.M., Astals, S., 2016. The role of additives on anaerobic digestion: a review. Renew. Sustain. Energy Rev. 58, 1486–1499.

Rotaru, A.-E., Shrestha, P.M., Liu, F., Shrestha, M., Shrestha, D., Embree, M., Zengler, K., Wardman, C., Nevin, K.P., Lovley, D.R., 2014. A new model for electron flow during anaerobic digestion: direct interspecies electron transfer to Methanosaeta for the reduction of carbon dioxide to methane. Energy Environ. Sci. 7 (1), 408–415.

Saha, S., Jeon, B.-H., Kurade, M., Govindwar, S., Chatterjee, P., Oh, S.-E., Roh, H.-S., Lee, S., 2019. Interspecies microbial nexus facilitated methanation of polysaccharidic wastes. Bioresour. Technol. 289, 121638.

Sousa, D., Smidt, H., Alves, M., Stams, A., 2007. Syntrophomonas zehnderi sp. nov., an anaerobe that degrades long-chain fatty acids in co-culture with Methanobacterium formicicum. Int. J. Syst. Evol. Microbiol. 57, 609–615.

Vanwonterghem, I., Jensen, P.D., Ho, D.P., Batstone, D.J., Tyson, G.W., 2014. Linking microbial community structure, interactions and function in anaerobic digesters using new molecular techniques. Curr. Opin. Biotechnol. 27, 55–64.

Wang, S., Li, Z., Gao, M., She, Z., Guo, L., Zheng, D., Zhao, Y., Ma, B., Gao, F., Wang, X., 2017. Long-term effects of nickel oxide nanoparticles on performance, microbial enzymatic activity, and microbial community of a sequencing batch reactor. Chemosphere 169, 387–395.

Wei, H., Wang, J., Hassan, M., Han, L., Xie, B., 2017. Anaerobic ammonium oxidation-denitrification synergistic interaction of mature landfill leachate in aged refuse bioreactor: variations and effects of microbial community structures. Bioresour. Technol. 243, 1149–1158.

Wu, J., Yang, Q., Luo, W., Sun, J., Xu, Q., Chen, F., Zhao, J., Yi, K., Wang, X., Wang, D., Li, X., Zeng, G., 2018. Role of free nitrous acid in the pretreatment of waste activated sludge: extracellular polymeric substances disruption or cells lysis? Chem. Eng. J. 336, 28–37.

Xia, T., Kovochich, M., Liong, M., Madler, L., Gilbert, B., Shi, H., Yeh, J.I., Zink, J.I., Nel, A.E., 2008. Comparison of the mechanism of toxicity of zinc oxide and cerium oxide nanoparticles based on dissolution and oxidative stress properties. ACS Nano 2 (10), 2121–2134.

Xiang, Y., Yang, Z., Zhang, Y., Xu, R., Zheng, Y., Hu, J., Li, X., Jia, M., Xiong, W., Cao, J., 2019. Influence of nanoscale zero-valent iron and magnetite nanoparticles on anaerobic digestion performance and macrolide, aminoglycoside, β-lactam resistance genes reduction. Bioresour. Technol. 294, 122139.

Xu, S., He, C., Luo, L., Lü, F., He, P., Cui, L., 2015. Comparing activated carbon of different particle sizes on enhancing methane generation in upflow anaerobic digester. Bioresour. Technol. 196, 606–612.

Xu, R., Yang, Z.-H., Wang, Q.-P., Bai, Y., Liu, J.-B., Zheng, Y., Zhang, Y.-R., Xiong, W.-P., Ahmad, K., Fan, C.-Z., 2018a. Rapid startup of thermophilic anaerobic digester to remove tetracycline and sulfonamides resistance genes from sewage sludge. Sci. Total Environ. 612, 788–798.

Xu, R., Yang, Z.-H., Zheng, Y., Liu, J.-B., Xiong, W.-P., Zhang, Y.-R., Lu, Y., Xue, W.-J., Fan, C.-Z., 2018b. Organic loading rate and hydraulic retention time shape distinct ecological networks of anaerobic digestion related microbiome. Bioresour. Technol. 262, 184–193.

Xu, R., Yang, Z.-H., Zheng, Y., Wang, Q.-P., Bai, Y., Liu, J.-B., Zhang, Y.-R., Xiong, W.-P., Lu, Y., Fan, C.-Z., 2019. Metagenomic analysis reveals the effects of long-term antibiotic pressure on sludge anaerobic digestion and antimicrobial resistance risk. Bioresour. Technol. 282, 179–188.

Yan, W., Shen, N., Xiao, Y., Chen, Y., Sun, F., Kumar Tyagi, V., Zhou, Y., 2017. The role of conductive materials in the start-up period of thermophilic anaerobic system. Bioresour. Technol. 239, 336–344.

Yang, Y., Chen, Q., Wall, J.D., Hu, Z., 2012. Potential nanosilver impact on anaerobic digestion at moderate silver concentrations. Water Res. 46 (4), 1176–1184.

Yin, Q., Miao, J., Li, B., Wu, G., 2017. Enhancing electron transfer by ferroferric oxide during the anaerobic treatment of synthetic wastewater with mixed organic carbon. Int. Biodeterior. Biodegrad. 119, 104–110.

Zhang, L., He, X., Zhang, Z., Cang, D., Nwe, K.A., Zheng, L., Li, Z., Cheng, S., 2017. Evaluating the influences of ZnO engineering nanomaterials on VFA accumulation in sludge anaerobic digestion. Biochem. Eng. J. 125, 206–211.

Zhang, L., Liu, H., Zheng, Z., Ma, H., Yang, M., Liu, H., 2018. Continuous liquid fermentation of pretreated waste activated sludge for high rate volatile fatty acids production and online nutrients recovery. Bioresour. Technol. 249, 962–968.

Zhang, K., Song, L., Dong, X., 2009. Proteiniclasticum ruminis gen. nov., sp. nov., a strictly anaerobic proteolytic bacterium isolated from yak rumen. Int. J. Syst. Evol. Microbiol. 60, 2221–2225.

Zhang, W., Wei, Q., Wu, S., Qi, D., Li, W., Zuo, Z., Dong, R., 2014. Batch anaerobic co-digestion of pig manure with dewatered sewage sludge under mesophilic conditions. Appl. Energy 128, 175–183.

Zhang, Y., Yang, Z., Xu, R., Xiang, Y., Jia, M., Hu, J., Zheng, Y., Xiong, W., Cao, J., 2019. Enhanced mesophilic anaerobic digestion of waste sludge with the iron nanoparticles addition and kinetic analysis. Sci. Total Environ. 683, 124–133.

Zhao, J., Wang, D., Liu, Y., Ngo, H.H., Guo, W., Yang, Q., Li, X., 2018. Novel stepwise pH control strategy to improve short chain fatty acid production from sludge anaerobic fermentation. Bioresour. Technol. 249, 431–438.

Zhen, G., Lu, X., Kobayashi, T., Li, Y.-Y., Xu, K., Zhao, Y., 2015. Mesophilic anaerobic co-digestion of waste activated sludge and Egeria densa: performance assessment and kinetic analysis. Appl. Energy 148, 78–86.

Zhen, G., Lu, X., Kobayashi, T., Kumar, G., Xu, K., 2016. Anaerobic co-digestion on improving methane production from mixed microalgae (Scenedesmus sp., Chlorella sp.) and food waste: kinetic modeling and synergistic impact evaluation. Chem. Eng. J. 299, 332–341.

Zheng, H.-S., Guo, W.-Q., Wu, Q.-L., Ren, N.-Q., Chang, J.-S., 2018. Electro-peroxone pretreatment for enhanced simulated hospital wastewater treatment and antibiotic resistance genes reduction. Environ. Int. 115, 70–78.